Prompt isothermal decay of thermoluminescence in MgB 4 O 7 :Dy, Na and LiB 4 O 7 :Cu, In dosimeters

ARTICLE · JANUARY 2016

READS

31

6 AUTHORS, INCLUDING:

George Kitis

Aristotle University of Thessaloniki

188 PUBLICATIONS **2,148** CITATIONS

SEE PROFILE

George S. Polymeris

Ankara University

101 PUBLICATIONS **557** CITATIONS

SEE PROFILE

Ioanna K. Sfampa

Aristotle University of Thessaloniki

10 PUBLICATIONS **34** CITATIONS

SEE PROFILE

V. Pagonis

McDaniel College

113 PUBLICATIONS **955** CITATIONS

SEE PROFILE

Radiation Measurements 84 (2016) 15–25

Contents lists available at ScienceDirect

Radiation Measurements

journal homepage: www.elsevier.com/locate/radmeas

Prompt isothermal decay of thermoluminescence in MgB_4O_7:Dy, Na and LiB_4O_7:Cu, In dosimeters

G. Kitis [a, *], G.S. Polymeris [b], I.K. Sfampa [a], M. Prokic [c, 1], N. Meriç [b], V. Pagonis [d]

[a] Aristotle University of Thessalonians, Physics Department, Nuclear Physics and Elementary Particles Physics Section, 54124, Thessaloniki, Greece
[b] Institute of Nuclear Sciences, Ankara University, 06100, Besevler, Ankara, Turkey
[c] Institute of Nuclear Sciences, Vinca, P.O. Box 522, 11001, Belgrade, Serbia
[d] McDaniel College, Physics Department, Westminster, MD 21157, USA

HIGHLIGHTS

- Isothermal decay of TL in MgB_4O_7:Dy, Na and LiB_4O_7:Cu, In is studied.
- The TL of LiB_4O_7:Cu, In is due to delocalized transitions.
- The TL of MgB_4O_7:Dy, Na is due to tunneling transitions.
- Recent TL expressions for delocalized and localized transitions are used to explain the results.

ARTICLE INFO

Article history:
Received 22 August 2015
Received in revised form
4 November 2015
Accepted 13 November 2015
Available online 1 December 2015

Keywords:
Thermoluminescence
Isothermal thermoluminescence
Lambert W function
TL-OSL dosimetry
Tunneling recombination

ABSTRACT

According to standard delocalized kinetic models of thermoluminescence (TL), when an irradiated sample is held at a high temperature T, the isothermal TL signal will decay with a characteristic thermal decay constant λ which depends strongly on the temperature T. This prediction of standard delocalized kinetic theory is investigated in this paper by studying two TL dosimeters, MgB_4O_7:Dy, Na and LiB_4O_7:Cu, In (hereafter MBO and LBO correspondingly). In the case of LBO it was found that the thermal decay constant λ of the main dosimetric TL peak follows exactly the predictions of standard delocalized kinetic theory. Furthermore, the thermal activation energy of the main peak evaluated by the isothermal decay method is in full agreement with values obtained from initial rise and glow curve fitting methods. However, in the case of MBO it was found that the thermal decay constant λ varies little with the isothermal decay temperature T. In order to explain these unusual results for MBO, the TL glow curves and isothermal decay curves were analyzed using analytical expressions derived recently from a radiative tunneling recombination model. Based on the different behavior of the two TL dosimeters, it is suggested that the isothermal decay of TL at high temperatures can be used to discriminate between radiative delocalized recombination and radiative localized recombination processes.

1. Introduction

Magnesium borate (MgB_4O_7) is a host matrix of interest for thermoluminescence (TL) dosimetry of ionizing radiation (McKeever et al., 1995). This material has been reported since the 1980s and 1990s as being attractive for dosimetry because of its low effective atomic number (Z_{eff}~8.4), which implies a small photon energy dependence (Prokic, 1980; Prokic, 1993; Prokic, 2007, 1993; Driscoll, 1981; Furetta et al., 2000; Lochab et al., 2007). Moreover, the possibility of developing neutron dosimeters based on these materials has also been suggested, because of the high neutron capture cross-section for ^{10}B (McKeever et al., 1995; Prokic, 1993; Price et al., 1998). Most of the literature on the TL properties of MgB_4O_7 is focused on its dosimetric properties when a variety of dopants is used.

Despite this high interest in the past, there has been no systematic study on the luminescence properties of MgB_4O_7. Recently Yukihara et al. (2014a) performed a systematic study of the TL properties of magnesium borate doped with lanthanides, in order to elucidate the thermally stimulated and recombination processes

* Corresponding author.
E-mail address: gkitis@auth.gr (G. Kitis).
[1] Dr M. Prokic has passed away last year.

http://dx.doi.org/10.1016/j.radmeas.2015.11.002
1350-4487/

in this material. Their results showed that different dopant were associated with TL peaks at different temperatures, involving different trapping mechanisms depending on the dopant element. These results stand in good agreement with Karali et al. (2002), who reported spectrally resolved TL curves which differ for MgB_4O_7 dosimeters variously doped with one or two rare earth (RE) dopant. These results provided further evidence that RE ions could form part of large complex defects, and/or long range interactions involving the charge trapping and recombination processes in TL.

Lithium tetraborate $Li_2B_4O_7$ is also a material of interest for TL dosimetry (McKeever et al., 1995), which has attracted a great deal of attention as a radiation resistant optical material and as a tissue-equivalent material for radiation dosimetry (Z_{eff}~7.25) (Park et al., 2003; Prokic, 2001a, b). In addition, lithium borate based crystals are convenient materials for neutron dosimetry due to the presence of Li and B (Tiwari et al., 2010). The original undoped material had some disadvantages like poor sensitivity, hygroscopic nature and relatively large fading rate. To improve its sensitivity, different dopant and preparation methods have been introduced by several researchers (Furetta et al. (2001); Prokic (2001a, b)). Single crystals, polycrystals and glass forms of Lithium tetraborate doped with rare-earth, copper and manganese ions are used effectively as TL dosimeters (Takenaga et al., 1980; Chandra and Bhatt, 1981; Kutomi and Takeuchi, 1996; Martini et al., 1996; Prokic, 2001a). The TL properties of $Li_2B_4O_7$ tend to vary with the synthesis method, preparation, dopant, and dopant concentrations (Wall et al., 1982). Generally, the TL curves tend to have a low temperature peak around 100 °C and a main dosimetric peak around 200 °C (Takenaga et al., 1980; Wall et al., 1982; Furetta et al., 2001; Prokic, 2001a, b). In some cases, a high temperature peak around 300 °C has been also reported (Kutomi and Takeuchi, 1986).

Both materials have regained scientific interest during the last few years, mostly for their possible use for passive temperature sensing using thermoluminescence (Yukihara et al., 2014a; Yukihara et al., 2014b; Doull et al., 2013, 2014), due to their low light sensitivity and, therefore, of potential application as a temperature sensor.

Among the various methods used to evaluate the kinetic parameters of a trap responsible for a TL glow-peak is the isothermal decay method (Chen and McKeever, 1997). There are two commonly used experimental versions of the isothermal decay technique. The first version is the residual isothermal decay method (RID) in which the irradiated sample is post irradiation annealed in a furnace and then the residual TL glow-curve is measured. The second version is the prompt isothermal decay (PID) in which TL is measured directly while the sample is held at a stable temperature in the TL reader. The basic measured parameter in an isothermal experiment is the thermal decay constant $\lambda=1/\tau$, where τ represents the thermal lifetime. According to standard TL models involving delocalized transitions, in the case of first order kinetics the parameter λ is expected to vary exponentially with the sample temperature T, according to $\lambda=s\,exp(-E/KT)$. In this expression s is the frequency factor, E is the thermal activation energy and T is the absolute temperature of the sample.

In a recent study Sfampa et al. (2014) reported a PID study of Durango apatite, which is a material exhibiting strong anomalous fading (AF). AF consists of the anomalous loss of TL and optically stimulated luminescence (OSL) signals after irradiation, which contradicts the predictions of standard luminescence kinetic theory, and is commonly attributed to a quantum tunneling effect (Wintle, 1977; Visocekas et al., 1976; Kitis et al., 1991). Sfampa et al. (2014) reported that the decay constant λ of the PID curves in Durango apatite was practically independent of isothermal temperature T, instead of the strong dependence expected from standard delocalized kinetic models. These authors analyzed successfully the PID curves of their experiment using analytical expressions for PID derived by Kitis and Pagonis (2013). These analytical expressions were based on the recently developed tunneling kinetic model of Jain et al. (2012).

The PID results of Sfampa et al. (2014) confirmed the prevalence of radiative tunneling recombination processes in Durango apatite. It is interesting to investigate whether this behavior is restricted in Durango apatite, or whether it exists in other natural material like feldspars, which also suffer from AF effects. Equally interesting is to investigate if a similar PID behavior exists in synthetic TL dosimeters.

The aims of this work are to investigate the behavior of PID signals in MgB_4O_7:Dy, Na and LiB_4O_7:Cu, In dosimeters, and to examine whether the PID behavior can be used to discriminate between delocalized radiative recombination and localized radiative tunneling recombination processes.

2. Experimental procedure

2.1. Sample details

The samples used in these experiments were *MgB_4O_7:Dy,Na* (hereafter termed as MBO) and *LiB_4O_7:Cu,In* (hereafter termed as LBO) obtained from the same production batch used by Furetta et al. (2000) and Kitis et al. (2000). Furetta et al. (2000) presented a complete dosimetric characterization of these materials, whereas Kitis et al. (2000) determined their characteristic kinetic parameters.

2.2. Apparatus and measurement conditions

TL measurements were carried out using a Risø TL/OSL reader (model TL/OSL–DA–15), equipped with a $^{90}Sr/^{90}Y$ beta particle source, delivering a nominal dose rate of 0.105 Gy/s. A 9635QA photomultiplier tube with a combination of Pilkington HA-3 heat absorbing and Corning 7-59 (320–440 nm) blue filter were used for light detection. All measurements were performed in a nitrogen atmosphere with a low constant heating rate of 2 °C/s, in order to avoid significant temperature lag, and the samples were heated up to the maximum temperature of 350 °C.

The PID method of isothermal luminescence is used in all experiments described in the present work.

2.3. Experimental protocols

The experimental procedure for the PID study of TL was performed according to the following protocol.

- Step 0: Test dose and TL measurement up to $T = 350$ °C for LBO and $T = 450$ °C for MBO at 2 °C/s.
- Step 1: The previously annealed aliquot is irradiated with a test dose TD = 1 Gy, in order to populate the traps and centers.
- Step 2: TL measurement up to a temperature T_{dec} at 2 °C/s. The sample is left to decay thermally for 500 s at this temperature, and the isothermal decay signal is measured.
- Step 3: After the end of the decay period, the sample is cooled down to room temperature.
- Step 4: TL measurement at 2 °C/s in order to obtain the residual TL glow curve (R-TL).
- Step 5: Repeat steps 1–4 for a new decay temperature T_{dec}.
- Step 6: Repeat step 0.

The peak maximum temperature (T_m) of LBO is 200 °C, whereas the corresponding value of T_m for MBO is 190 °C. In the case of LBO the sample was pre-heated before step 2 at 2 °C/s, up to a

temperature of 150 °C, in order to erase a low temperature peak present in the data.

For both LBO and MBO the lowest isothermal decay temperature T_{dec} was 90 °C, and the highest value of T_{dec} was 170 °C, i.e ~ 20–30 °C below the T_m. Higher T_{dec} values were avoided for the following reasons:

(a) The percentage of trapped electrons thermally released during the TL readout up to T_{dec} must be kept in a relatively low level, in order for the isothermal decay to represent accurately the decay of the population of trapped electrons.
(b) The thermal decay constant λ is expected to depend very strongly on the isothermal temperature T_{dec}, so that at temperatures close to or higher than the peak maximum temperature T_m the isothermal decay will become extremely short lived and difficult to measure.

The positions of the prompt isothermal TL decay temperatures T_{dec} on the glow-curve of each dosimeter can be seen in Fig. 1.

The protocol run in single aliquot mode for both materials. Step 0 and step 6 measure the initial and final sensitivity of each sample. The sensitivity tests in steps 0 and 6 were also applied two more times after the T_{dec} s of 120 and 150 °C. In all cases the results verified the already known excellent stability of these materials (Furetta et al., 2000; Kitis et al., 2000) to repeated irradiation–TL readout cycles. Negligible sensitivity changes were observed for all samples.

3. Preliminary remarks

The results obtained in the present work show appreciable differences between the two dosimeters. Fig. 1 shows the residual TL (R-TL) glow curves measured after prompt isothermal decay at various decay temperatures T_{dec}, which are noted as perpendicular bars along the first R-TL glow-curve. It is clear that the R-TL glow-curves for LBO decrease as a function of T_{dec}, in a manner very different from that of MBO. Specifically, as the isothermal decay temperature T_{dec} is increased, the R-TL glow-curves for MBO shift systematically towards higher temperatures, while the higher temperature part of the glow curves remains unchanged. This behavior is exactly similar to that reported by Pagonis et al. (2014) and Sfampa et al. (2015) for feldspar, which are materials exhibiting the anomalous fading effect. Furthermore, such a behavior is predicted by the localized tunneling recombination model by Jain et al. (2012) proposed to explain the anomalous fading in feldspar. By contrast, the R-TL glow curves for LBO in upper Fig. 1 retain their shape as T_{dec} is increased, and there is no systematic shift of the peak maximum. This behavior of LBO glow curves is consistent with standard kinetic models of TL.

However, the differences between the two materials become even more prominent in their PID curves shown in Fig. 2. According to the standard kinetic models the decay constant of the PID curves depends exponentially on the T_{dec}. In the case of LBO the PID curves seem to fulfill this property, because they show a strong dependence of the PID rate on T_{dec}. As T_{dec} is increased, the isothermal decay signals for LBO decrease by about two orders of magnitude. On the other hand the decay rates of the PID curves of MBO in Fig. 2 are negligible within a broad region of temperatures T_{dec}. Therefore, they do not follow the predictions of standard TL kinetic theory. As T_{dec} is increased, the isothermal decay signals for MBO decrease slightly above one order of magnitude. Furthermore, the experimental behavior of PID curves of MBO is exactly similar to the

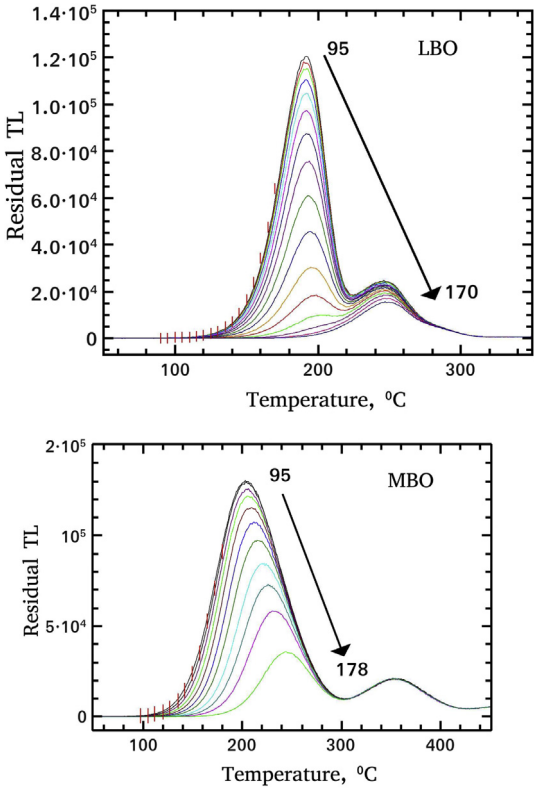

Fig. 1. Residual TL glow-curves of LBO and MBO after prompt isothermal decay for 500 s at the temperatures shown by the arrows. The perpendicular bars show the position of the decay temperatures on the first R-TL glow curve.

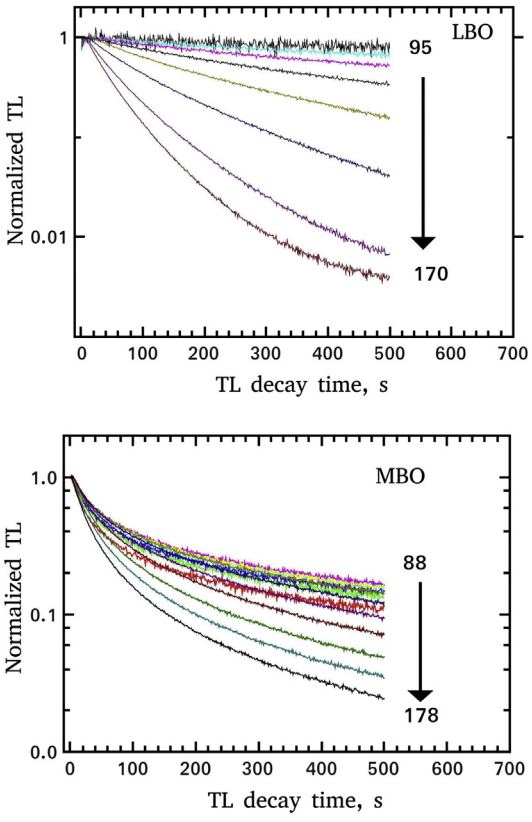

Fig. 2. Series of prompt isothermal decay curves of LBO samples (upper figure) and MBO samples (lower figure), for a broad region of decay temperatures.

recently reported PID results on Durango apatite, which exhibits strong anomalous fading, obtained by Sfampa et al. (2014), using the same exactly protocol as in the present work. Concerning the fading of different batches of MBO dosimeters at room temperature, it was found to be 10% in three months by Furetta et al. (2000) and 40% in fifteen days by Furetta et al. (1999).

From these preliminary remarks based on Figs. 1 and 2, it became clear that since the standard kinetic models can not predict the non-exponential dependence of the PID curves of MBO on T_{dec}, alternative models should be considered for analysis of MBO experimental data. The detailed methods of analysis used in this work will be described in the next section.

4. Methods of analysis

The following three different types of analytical expressions have been used in the present work to analyze the experimental results:

1. The TL glow curves and isothermal decay curves (PID) for LBO were analyzed by assuming that the TL and isothermal decay processes follow standard general order kinetics. These equations are presented in Section 4.1.
2. As a further check of the results obtained using general order kinetics, the experimental data for LBO were also analyzed using analytical expressions for TL and PID, which were derived from the solution of the system of differential equations for the one trap one recombination center model (OTOR) (Kitis and Vlachos, 2012). These equations are described in Section 4.2.
3. In the case of MBO it was found that standard general order kinetics could not describe the experimental data. In this material the experimental data were analyzed using analytical expressions for TL and PID derived from the model by Jain et al. (2012). These equations are described in Section 4.3.

It must be noted that in this paper the term delocalized model represents only the OTOR model, and not to more advanced models like the interactive or non interactive multitrap system models (IMTS and NMTS models correspondingly). Similarly, the term localized model in this paper represents only the localized tunneling recombination model by Jain et al. (2012).

4.1. TL and PID expressions based on general order kinetics (GOK)

The experimental TL glow-curves were fitted using the well-known general order kinetic equation by May and Partridge (1964), in the form proposed by Kitis et al. (1998) (see for example Chen and McKeever (1997)). In the case of general order kinetics, Kitis et al. (1998) derived the following expression:

$$I(T) = I_m b^{\frac{b}{b-1}} exp\left(\frac{E}{kT}\frac{T-T_m}{T_m}\right)\left[Z_m + (b-1)(1-\Delta)\left(\frac{T^2}{T_m^2}exp\left(\frac{E}{kT}\frac{T-T_m}{T_m}\right)\right)\right]^{-\frac{b}{b-1}}. \quad (1)$$

In this expression E is the activation energy (in eV), T the temperature (in K), k the Boltzmann constant ($eV\,K^{-1}$), I_m the maximum intensity of the glow peak, T_m the temperature at peak maximum (in K). b is the kinetic order of the TL process, $\Delta = 2kT/E$ and $Z_m = 1+(b-1)2kT_m/E$. The advantage of using these equations to describe the TL glow curve is that they involve two quantities, which are measured experimentally, namely the maximum TL intensity and the corresponding temperature (I_m and T_m). The activation energy E and the kinetic order b are treated in these expressions and during the computerized fitting procedure as adjustable parameters.

The experimental PID curves were analyzed using the following general order kinetics expression for isothermal TL (Chen and McKeever (1997)):

$$I(t) = I_0\left[1 + (b-1)\frac{t}{\tau}\right]^{-\frac{b}{b-1}}, \quad b \neq 1. \quad (2)$$

where $I(t)$ is the intensity of the luminescence signal as a function of time, $\tau = 1/\lambda$ (s) is the lifetime for isothermal decay, and b is the order of kinetics. The kinetic order b was left to vary freely in the region $1.05 < b < 2.05$.

4.2. TL and PID expressions based on the solution of the OTOR model

The case of general order kinetics can be considered as an empirical approach to the elementary OTOR model (see for example the recent work by Sadek et al. (2015)). These authors found that for retrapping coefficients A_n lower than the recombination coefficient A_m ($A_n \leqq A_m$), the greatest deviation between OTOR generated TL peaks and general order kinetics is less than 4% of the TL intensity at all temperatures along the glow curve. This 4% theoretical deviation between these OTOR cases and GOK is rather small, so the empirical general order expression has shown to be very effective in analyzing experimental TL glow-curves. However, in cases where $A_n > A_m$, it was found that general order kinetics fails in most cases to describe an OTOR generated TL peak.

Recent work by Kitis and Vlachos (2012) showed that analytical solutions of the system of differential equations for the OTOR system can be obtained by using the Lambert function $W(z)$. The expressions derived by Kitis and Vlachos (2012) are advantageous, because the analytical solution of the OTOR model gives a general equation which can describe many commonly used stimulation modes for luminescence signals. Specifically these authors found that the same equations can describe TL, isothermal TL, continuous wave optical stimulated luminescence (CW-OSL), linearly modulated OSL (LM-OSL), and TL measured using variable heating rates (as for example in the case of the exponential heating rate used in stable temperature hot gas TL readers).

The original equation derived by Kitis and Vlachos (2012) as a solution of the OTOR model is:

$$I(T) = \frac{N\,R}{(1-R)^2}\frac{p(t,T)}{W(z)+W(z)^2} \quad (3)$$

where N is the total concentration of trapping states and $W(z)$ is the Lambert W function (Corless et al., 1996), and $R = A_n/A_m$ with A_n, A_m being the retrapping and recombination coefficients correspondingly. As discussed by Kitis and Vlachos (2012) and by Sadek et al. (2015), this equation is most useful for fitting experimental data

for cases $R < 1$. The function $p(t,T)$ in Eq. (3) describes the stimulation mode used during the experiments, which for the case of TL is $p(T)=sexp(-E/kT)$.

The argument z of the Lambert function $W(z)$ for the case of TL is:

$$z = exp\left(\frac{R}{e}1 - R - ln\left(\frac{1-R}{R}\right)\frac{s}{\beta(1-R)}\int_{T_0}^{T} e^{-\frac{E}{kT}}dT\right) \quad (4)$$

In the case of TL the original Eq. (3) was transformed by Sadek et al. (2015), so that the parameters N and s were replaced by the maximum TL intensity of the peak I_m and by the temperature of the peak maximum T_m. This is a very useful substitution, since these two quantities I_m and T_m can be obtained directly and accurately from the experimental TL glow curves.

The final equation given by Sadek et al. (2015) is:

$$I(T) = I_m exp\left(-\frac{E}{k\,T}\cdot\frac{T_m - T}{T_m}\right)\cdot\frac{W(z_m) + W(z_m)^2}{W(z) + W(z)^2} \quad (5)$$

where z is now approximated by the expression:

$$z = exp\left(\frac{R}{1-R} - log\left(\frac{1-R}{R}\right) + \frac{E\,exp(E/kT_m)}{kT_m^2(1 - 1.05R^{1.26})}\cdot F(T,E)\right) \quad (6)$$

and z_m is the value of z for $T = T_m$.

Equations (5) and (6) are the analytical equations used to fit the experimental TL glow curves, with the two adjustable fitting parameters being the activation energy E and the ratio R (with $R < 1$).

The function $F(T,E)$ in this expression is the exponential integral appearing in TL models and is expressed in terms of the exponential integral function $Ei[-E/kT]$ as (Chen and McKeever, 1997; Kitis et al., 2006):

$$F(T,E) = \int_{T_0}^{T} e^{-\frac{E}{kT}}dT = T\,exp\left(-\frac{E}{k\,T}\right) + \frac{E}{k}Ei\left[-\frac{E}{k\,T}\right] \quad (7)$$

For the case of PID experiments the function $p(t,T)$ in Eq. (3) is given by $p(t)=\lambda=sexp(-E/kT_{dec})$, where T_{dec} is the isothermal decay temperature. The argument z of the Lambert $W(z)$ function for PID processes takes the form:

$$z = exp\left(\frac{R}{1-R} - ln\left(\frac{1-R}{R}\right) + \frac{\lambda\,t}{1-R}\right) \quad (8)$$

Equations (3) and (8) are the analytical equations used to fit the experimental PID glow curves, with the two adjustable fitting parameters being the decay constant λ and the ratio R (with $R < 1$).

The application of the Lambert function $W(z)$ is quite complicated when one has to use analytical approximations for it (Kitis and Vlachos, 2012). On the other hand its application is very simple in software packages (for example MATHEMATICA, MATLAB) which contain it as a built-in function, similar to any other transcendental function like sine, cosine etc. In the present work the ROOT data Analysis Framework was used (ROOT, 2015). All fittings were performed using the MINUIT program (MINUIT, 2015) released in ROOT, which is a physics analysis tool for function minimization. The Lambert function $W(z)$ and the exponential integral function $Ei[-E/kT]$ are implemented in ROOT through the GNU scientific library (GNU GSL) (GNU, 2015).

4.3. TL and PID expressions based on the localized tunneling model by Jain et al. (2012)

The PID curves for sample MBO shown in Fig. 2 show characteristics, which are very similar to those observed in Durango apatite by Sfampa et al. (2014). These authors found that the PID decay constant λ did not follow the expected exponential dependence as a function of the decay temperature T_{dec}, and used a different approach based on a localized tunneling recombination model (Jain et al., 2012; Kitis and Pagonis, 2013). The same model will be used in this paper to analyze the PID curves for the MBO.

Jain et al. (2012) presented a new general kinetic model which quantifies localized electronic recombination of donor-acceptor pairs in luminescent materials. The main physical assumption in the model is the presence of a random distribution of hole traps in the luminescent volume, and an associated range of random nearest-neighbor recombination probabilities. Stimulated recombination takes place only via the excited state of the electron trap, by either optical or thermal stimulation. The concentration of holes is assumed to be much larger than the concentration of electron traps, and an electron can tunnel only to its nearest hole.

Recently, Kitis and Pagonis (2013) obtained analytical solutions of the set of differential equations in the model of Jain et al. (2012) by using certain mathematical and physical simplifications. These authors presented analytical expressions describing thermally and optically stimulated luminescence signals within this model. The following analytical equation for TL glow curves was derived by Kitis and Pagonis (2013), within the framework of the tunneling recombination model by Jain et al. (2012):

$$L(T) = 3n_0\rho' zse^{-\frac{E}{kT}}\,e^{-F(T)}\,e^{\left(-\rho'\left(F(T)^3\right)\right)} \quad (9)$$

where the function $F(T)$ for TL processes is given by

$$F(T) = ln\left[1 + \frac{z\,s\,k\,T^2}{\beta\,E}e^{-\frac{E}{kT}}\left(1 - \frac{2k\,T}{E}\right)\right] \quad (10)$$

In these equations n_0 is the initial concentration of trapped electrons, z a constant, E the activation energy, s the frequency factor, k is the Boltzmann constant, ρ' a dimensionless parameter representing the normalized donor-acceptor density and T the temperature of the sample given by $T = T_0+\beta t$ for an experiment carried out with a linear heating rate β.

The application of Eq. (9) in fitting experimental data depends strongly on the initial values of its free parameters. Kitis and Pagonis (2014) transformed it as in the case of Eq. (5), i.e they replaced the initial parameters n_0 and s by the experimentally known quantities I_m and T_m. The transformed equation given by Kitis and Pagonis (2014) is:

$$L(T) = L_m\,exp\left(-\frac{E\,(T_m - T)}{k\,T\,T_m}\right)\cdot\left(\frac{F}{F_m}\right)^2\cdot\frac{exp\left(-\left(\rho' F_m^3 + F_m\right)\right)}{exp\left(-\left(\rho' F^3 - F\right)\right)} \quad (11)$$

with the function $F(T)$ given by Equation

$$F(T) = ln\left(1 + \frac{1}{f_m}\frac{T^2}{T_m^2}exp\left[-\frac{E(T_m - T)}{kT\,T_m}\right]\left(1 - \frac{2kT}{E}\right)\right) \quad (12)$$

and F_m is the value of $F(T)$ at $T = T_m$. The parameters f_m and F_m are related to each other by the equation:

$$F_m = ln\left(1 + \frac{1}{f_m}\left(1 - \frac{2kT_m}{E}\right)\right) \quad (13)$$

Eq. (11) is the fitting equation used to fit PID curves in the localized model, with the free fitting parameters E and f_m (or F_m), and with the quantities I_m, T_m known from the experimental data. The exact procedure for fitting experimental TL glow curves with these analytical equations is given in Kitis and Pagonis (2014). Although this equation seems more complicated than the original Eq. (9), it has been proved to be extremely powerful in analyzing experimental TL glow-curves (see for example Pagonis et al. (2014) for analysis of experimental TL glow curves in feldspars).

Using the condition for the TL maximum, Kitis and Pagonis (2014) obtained the following expression for the dimensionless density parameter ρ':

$$\rho' = \frac{f_m F_m e^{F_m} - F_m + 2}{3F_m^3} \tag{14}$$

For the case of PID curves, the corresponding equation for the isothermal intensity was given by Kitis and Pagonis (2013):

$$L(t) = \frac{3\, n_0 \rho' F(t)^2\, e^{-\rho' (F(t))^3}}{1 + z\, \lambda\, t} \tag{15}$$

with

$$F(t) = ln(1 + z\, \lambda\, t) \tag{16}$$

This is the equation used to fit the PID curves for sample MBO, and the free fitting parameters are the isothermal decay constant λ and the dimensionless density parameterρ'.

5. Results and discussion

In the present work all experimental results were analyzed using a computerized glow curve deconvolution (CGCD) procedure using the MINUIT program (MINUIT, 2015), which is a physics analysis tool for function minimization, released in ROOT (ROOT, 2015).

The goodness of fit was tested using the figure of merit (FOM) (Balian and Eddy, 1977) which is given by

$$FOM = \sum_i \frac{|Y_{Exper.} - Y_{Fit}|}{A}, \tag{17}$$

where $Y_{Exper.}$ is the experimental glow-curves, Y_{Fit} the fitted glow curves and A is the area of the fitted glow-curves.

5.1. LBO

5.1.1. Analysis of residual-TL glow curves (R-TL)

The TL glow-curve of LBO was analyzed by Kitis et al. (2000) using a two step procedure. In the first step the glow-curve was analyzed, with the goal to achieve the best fit with the lowest possible number of TL peaks. In the second step the analysis of the TL glow-curve was based on activation energy values obtained by the T_{stop}-T_{max} method, and also from the variable heating rate method (VHR). In the case of LBO only minor differences were observed between the two steps. It must be noted that during the VHR method it was found that the integrated signal of the main peak was increased by a factor of two by varying the heating rate between 1 and 20 °C/s.

All R-TL glow-curves shown in Fig. 1 were deconvolved using the general order kinetics Eq. (1) (Kitis et al., 1998), as well as Eq. (5), which is based on the OTOR solution using the Lambert W function. An example of a deconvolved TL glow-curve of LBO is shown in Fig. 3. This figure has to be explained in more detail. First of all, both

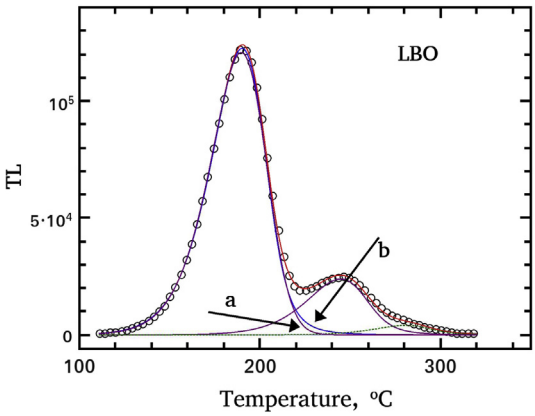

Fig. 3. CGCD analysis of TL glow-curve for LBO using general order kinetics Eq. (1) and the expression Eq. (5) based on the OTOR solution. Both equations gave excellent fit. The figure contains the main TL peak resulting from both equations. The differences between the two expressions are restricted at the high temperature end of the glow-peak indicated by the arrows. Arrow (a) represent general order kinetics and arrow (b) represents the OTOR solution function.

the general order kinetics Eq. (1), as well as the alternative Eq. (5) derived from the OTOR solution, gave excellent fits to the experimental glow-curves, with FOM values of around 1%. For comparison reasons, the figure shows the analysis of the main peak using both types of equations. Arrow (a) shows the result from the general order equation, whereas arrow (b) shows the result using the equation based on the solution of the OTOR model. As it seen in this figure, Eq. (1) and Eq. (5) differ only at the very high temperature part of the glow peak, with the general order peak tending much faster to zero. It must be noted that this situation is exactly similar with the results obtained from a comparison between general order and mixed order kinetics reported by Kitis et al. (2000).

The activation energy E of the main TL peak was evaluated by application of three different methods: by the initial rise method on the rising part of the R-TL glow-curves, by the CGCD analysis using the GOK Eq. (1), and by using the OTOR solution Eq. (5). The resulting values from these three types of analysis are shown in Fig. 4, with all three methods giving very similar E-values.

The kinetic order obtained from the fit using the general order equation was $b = 1.16 \pm 0.014$, whereas the parameter R resulting from the fit with Eq. (5) was $R = A_n/Am = 0.11 \pm 0.02$. These values of b and R correspond to the shape of a TL peak very close to first

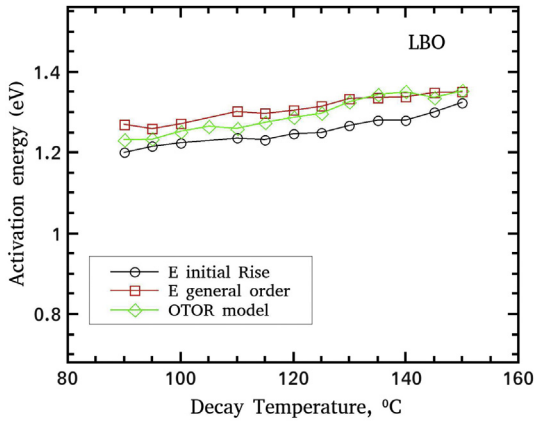

Fig. 4. Activation energies of the main peak of LBO evaluated using the initial rise method, the CGCD analysis using general order kinetics and the CGCD analysis using OTOR solution function.

order kinetics.

Concerning the second TL peak around 250 °C, the mean values of the fitting parameters from the CGCD analysis are: (a) General order method: $T_m = 244 \pm 0.5$ °C, $E = 1.44 \pm 0.05$ *eV* and $b = 1.3 \pm 0.1$ (b) OTOR solution method: $T_m = 245 \pm 0.5$ °C, $E = 1.54 \pm 0.1$ *eV* and $R = 0.13 \pm 0.04$. The net conclusion is that there is excellent agreement between the conventional method based on general order kinetics, and the TL peak expressions based on the OTOR solution function.

The kinetic parameters of the third TL peak around 285 °C are not given, due to the very low statistics of this peak relative to the other two.

All attempts to fit the R-TL glow-curves of LBO using the TL tunneling expression Eq. (11), failed. This was expected, because the shape of the experimental TL glow curves for LBO are very close to first order kinetics, while the lowest symmetry factor (μ_g) predicted by Eq. (11) is greater than 0.52 (Kitis and Pagonis, 2014), which corresponds to a kinetic order value of $b = 2$.

5.1.2. Analysis of PID curves

An example of a PID curve for LBO analyzed using the GOK Eq. (2) and also with Eqs. (3) and (8) based on the OTOR solution function, is shown in Fig. 5. Both equations gave identical fits. The values of the kinetic order b and the parameter R are shown in Fig. 6. At low PID temperatures the statistics are very poor, so an accurate evaluation of the kinetic parameters is not possible. This is the reason that the kinetic order b and parameter R do not follow the same trend, since the kinetics order tends steadily to the value of second order. However, for PID temperatures above 130 °C the fitting provides accurate values of the kinetic order b and of the parameter R, so Fig. 6 shows clearly that these two parameters follow an identical evolution as a function of the isothermal decay temperature.

The values of the lifetime τ evaluated from fitting all PID curves, allow the evaluation of the activation energy from the slope of the $ln(\tau)$ versus $1/kT_{dec}$ plot shown in Fig. 7. As it is seen, the τ values from general order kinetics and from Eqs. (3) and (8) using the OTOR solution function coincide for PID temperatures above 120 °C. The resulting value of the activation energy from both plots is $E = 1.17 \pm 0.01$ eV, which is very close to the values shown in Fig. 4. All these activation energy values are also in close agreement with the values reported by Kitis et al. (2000).

All attempts to fit the PID curves of LBO using the tunneling Eq. (15) failed. In conclusion, the experimental data for LBO has been shown to be in good agreement with the predictions of the standard kinetic theory of TL. Furthermore, very good agreement is obtained between the parameters obtained by analyzing PID TL curves and by fitting TL glow curves.

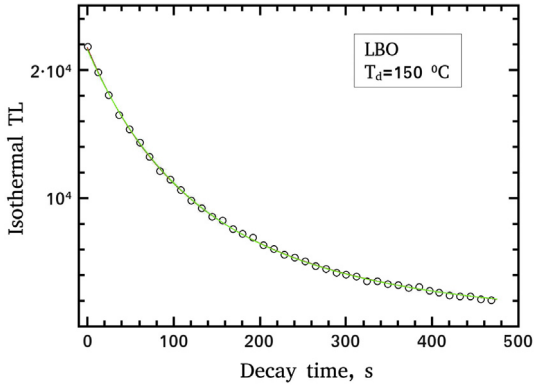

Fig. 5. An example of a PID curve for LBO analyzed using the GOK Eq. (2) and also with Eqs (3) and (8) based on the OTOR solution function. Both equations gave identical fits. The analysis gives the values of $\tau = s^{-1} exp(E/kT_d)$ as a function of decay temperature T_{dec}, which were used to evaluate the activation energy using PID method (see Fig. 7).

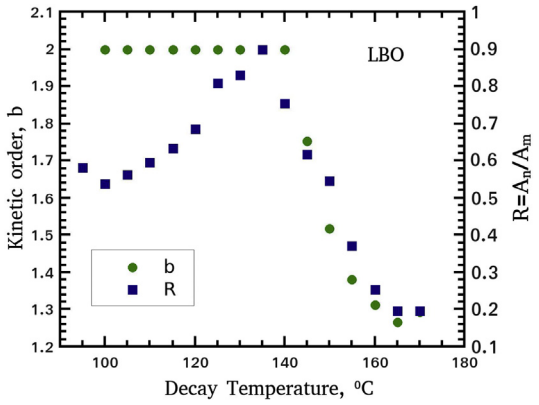

Fig. 6. Analysis of isothermal decay data for LBO. The kinetics order b is obtained from the general order isothermal expression Eq. (2), and the parameter $R=A_n/A_m$ is obtained from the OTOR solution Eq. (5), as a function of the decay temperature.

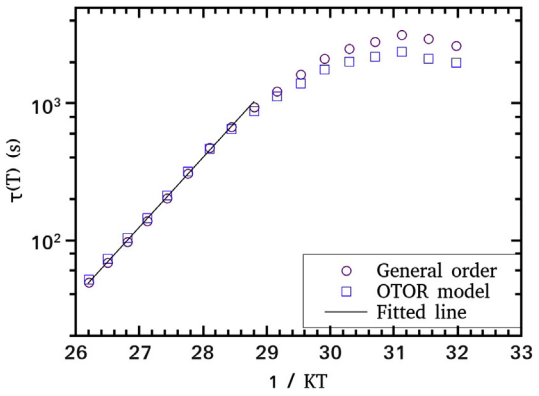

Fig. 7. Evaluation of the activation energy of the main TL peak of LBO using the values of τ resulting from the analysis of the PID curves using general order kinetics and OTOR solution equations. The activation energy is evaluated from the slope of $\ln(\tau)$ versus $1/kT_{dec}$ plot.

5.2. MBO

5.2.1. Analysis of R-TL glow curves

The TL glow-curve of MBO was analyzed by Kitis et al. (2000) using a two step procedure. In the first step the glow-curve was analyzed, with the goal of achieving the best fit with the lowest possible number of TL peaks. In the second step the analysis of the TL glow-curve was based on activation energy values obtained by the T_{stop}-T_{max} method and by the variable heating rate method (VHR). During the VHR method it was found that the integrated signal of the main peak was decreased by less that 10% between the heating rates of 1 and 20 °C/s. In the case of this material (MgB_4O_7:Dy,Na) important differences were observed between the two steps. In the first step the main peak was approached as a single general order TL peak, and the result was a poor fit. In the second step based on the results of the T_{stop}-T_{max} method, five peaks were used to obtained a very good fit of the main TL peak.

In the present study a CGCD analysis will be applied to MBO glow-curves looking for the best fit with the lowest possible number of TL peaks, i.e. by following the first method presented in Kitis et al. (2000). The aim of the present work is different from the

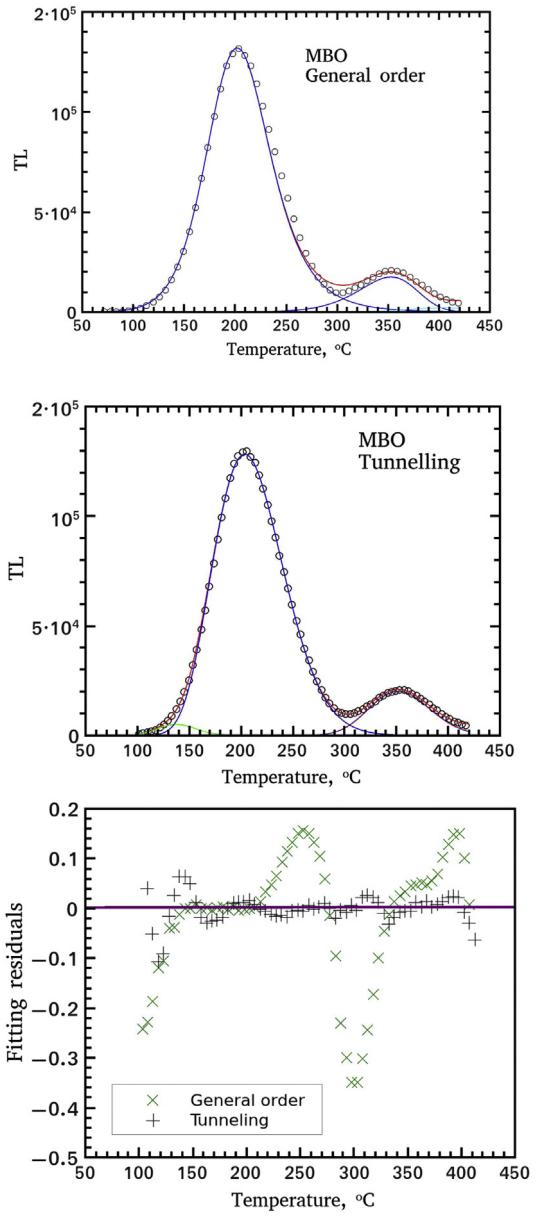

Fig. 8. Comparison of the CGCD analysis of the TL glow-curve of MBO using general order kinetics (upper figure) and the tunneling expression given by Eq. (11) (lower figure). The residuals of both fitting evaluated through $100^{*}(TL_{exp.}-TL_{fit.})/TL_{exp.}$ are shown in the down figure. The *x* symbol represents the fit with general order whereas the + symbol represents the fit with tunneling equations. It is clear that the fitting using the tunneling equation is superior than that of the general order equation.

older work on these materials, and includes a comparison between TL analytical equations originating from delocalized and localized recombination models.

The CGCD analysis of the TL glow-curves of MBO was attempted using three different TL peak expressions. The upper part of Fig. 8 is an example of a fit using either conventional general order kinetics (Kitis et al., 1998), or by using the OTOR solution expression given by Eq. (5). Both expressions gave identical results, but both of them failed to fit the glow-curve using a single TL peak in the temperature region of the main peak centered at 190 °C. The example glow-curve corresponds to the R-TL glow-curve measured after the PID measurement at 95 °C. The FOM values are ~ 6%. The fitting of the R-TL glow-curves obtained at higher PID temperatures gave again FOM values greater than 6%.

After the fitting failure of these TL expressions obtained from the standard TL kinetic models, all R-TL glow-curves were fitted using the TL peak expression given by Eq. (11), which is derived from the localized tunneling model of Jain et al. (2012). A fitting example is shown in the middle part of Fig. 8. The FOM values obtained were in the range 0.8−1.5%, which are obviously highly improved relative to the FOM of about 6% obtained by using general order kinetics and by using the OTOR solution expression Eq. (5). The improvement becomes more clear by the comparison of the fitting residuals from the two methods shown in the lower Fig. 8.

The activation energy of the main peak was evaluated as in the case of LBO, by applying the initial rise method on the rising part of the R-TL glow-curves. It is also evaluated from CGCD analysis using Eq. (11). Both sets of values are shown in Fig. 9. As it is seen, the values obtained by the initial rise method are about 10% higher. It is not clear what causes this 10% discrepancy, and it is conceivable that it is due to systematic errors introduced by the least squares fitting routines.

In the framework of the model by Jain et al. (2012), the values of the parameter ρ' shown in Fig. 10 are of special importance. Basically, the model by Jain et al. (2012) requires this parameter to be constant. Fig. 10 shows that this requirement is more or less fulfilled up to a T_{dec} of 140 °C, and that the value of ρ' increases at higher decay temperatures T_{dec}. The horizontal straight line with error bars corresponds to the mean value and its standard deviation, i.e. $\rho' = 0.01 \pm 0.002$, and provides an indication of the range within which this parameter can be considered a constant.

Concerning the second TL peak around 355 °C, the mean values of the trapping parameters resulting from CGCD analysis of all R-TL glow-curves are: $E = 1.31 \pm 0.06$ eV, $T_m = 351 \pm 1$ °C and $\rho'=0.023 \pm 0.002$.

5.2.2. *Analysis of PID curves with general order kinetics Eq. (2) and with the OTOR Eqs. (3) and (8)*

The analysis of PID curves for MBO samples requires two isothermal components for an acceptable fit. All PID curves were fitted using (a) general order kinetic Eq. 2, (b) OTOR equation Eqs. (3) and (8) and (c) the tunneling Eq. (15). Fitting examples for the first two methods are shown in Fig. 11, and in all cases the fits were excellent. Furthermore, in the case of PID curves for T_{dec} above 110 °C (when the statistics becomes satisfactory), the FOM values dropped down below 1%.

The values of the fitting parameters are:

Component 1: Mean value of kinetic parameters for T_{dec} between 100 and 170 °C (a) using general order kinetics, $\tau = 62 \pm 5\,s$ and $b = 1.93 \pm 1.15$. (b) using Eqs. (3) and (8), τ=62.±7 s and

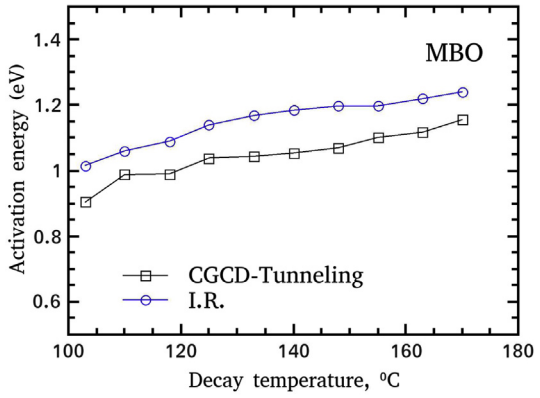

Fig. 9. Activation energies of the main TL peak of MBO evaluated from the initial rise method and CGCD analysis using the tunneling Eq. (11).

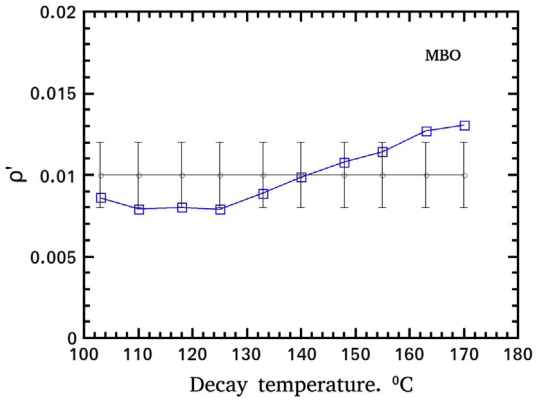

Fig. 10. The value of the parameter ρ' of the main TL peak of MBO resulting from the CGCD analysis using Eq. (11). The horizontal straight line with error bars corresponds to the mean value and its standard deviation $\rho' = 0.01 \pm 0.002$.

$R = 0.81 \pm 0.04$. Therefore, the two methods of analysis gave essentially the same results.

Component 2: This component becomes appreciable for $T_{dec} > 125$ °C. In the PID temperature region 125–170 °C, the Arrhenius plot of $\ln(\tau)$ versus $1/kT_{dec}$ was a very good straight line with its slope representing the activation energy, i.e. (a) general order kinetics Eq. (2): $E = 0.37 \pm 0.02$ eV and (b) OTOR Eqs. (3) and (8): $E = 0.35 \pm 0.01$ eV.

The conclusions are:

Conclusion 1: The complete independence of the value of τ from on temperature for the first component verifies the preliminary remarks in Section 3. This is a result in complete disagreement with the standard kinetic models. Note the value of τ=62 ± 5 *s*.

Conclusion 2: The τ of the second component shows a very weak dependence on temperature, which, however, is far from that expected according to the standard kinetic models. However, the standard kinetic models gave the correct *E* value in the case of LBO, as discussed in Section 5.1.2.

5.2.3. *Analysis of PID with the tunneling model Eq. 15*

The results of fitting the PID curves using the tunneling Eq. (15) are shown at the lower part of Fig. 11, and can be summarized as follows:

Component 1. As in the case of the empirical general order kinetics and Eqs. (3) and (8) presented above, the lifetime does not show any temperature dependence on T_{dec} interval between 100 and 150 °C. Its mean value is found at τ=0.38±0.03 *s* sec. However, at the highest T_{dec} region and specifically between 140 and 170 °C, the lifetime becomes temperature dependent. The Arrhenius plot of $\ln(\tau)$ versus $1/kT_{dec}$ was a very good straight line with slope E= 0.34 ± 0.04 eV.

Component 2. The lifetime does not show any temperature dependence in the interval of T_{dec} between 100 and 150 °C, and its mean value is $\tau = 6.4 \pm 1.05$ *s*. However, at the highest T_{dec} values in the interval between 140 and 170 °C the lifetime becomes temperature dependent. The Arrhenius plot of $\ln(\tau)$ versus $1/kT_{dec}$ was a very good straight line with slope $E = 0.35 \pm 0.04$ eV.

The conclusions from these results are summarized as follows:

Conclusion 1: Both components have a temperature independent tunneling lifetime τ, for a broad range of temperatures T_{dec}.

Conclusion 2: Both components show a weak temperature dependent lifetime τ at isothermal temperatures higher than 140 °C.

Conclusion 3: The tunneling lifetimes of 0.38 s and 6.4 s are much lower that the corresponding lifetime of 62 s from standard kinetic models presented in the previous Section 5.2.2.

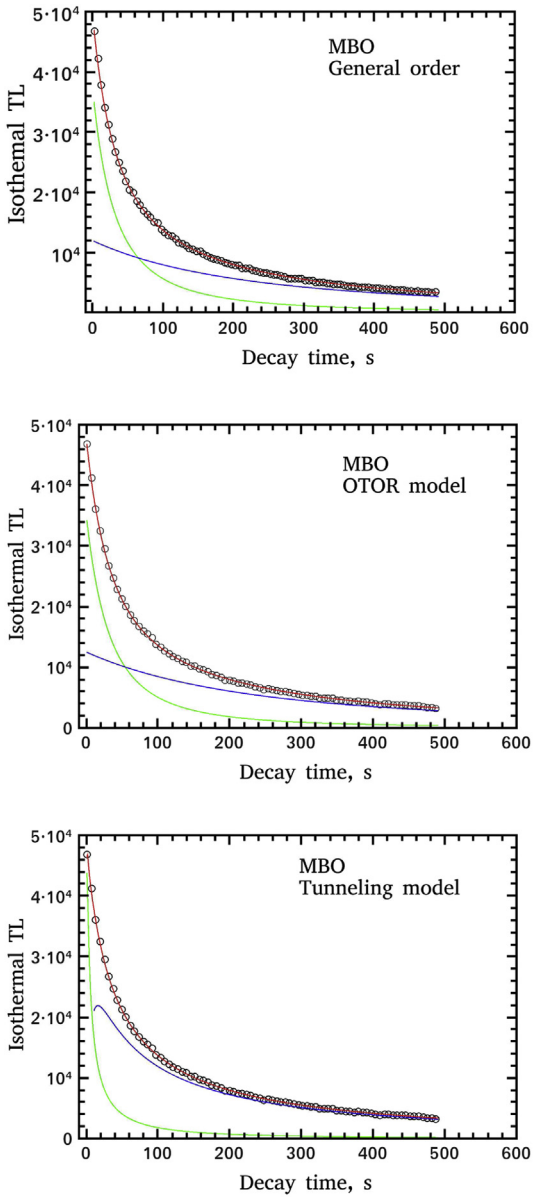

Fig. 11. Examples of component resolved PID curves of MBO analyzed using the general order kinetics Eq. (2) (upper figure), by the OTOR solution Eqs (3) and (8) (middle figure), and by the localized tunneling recombination model Eq. (15) (lower figure).

Conclusion 4: The same activation energy of around 0.35 eV is obtained from both OTOR and tunneling models, despite the very different mathematical expressions used to analyze the PID curves.

Based on the conclusions of Sections 5.2.2 And 5.2.3, it is suggested that the behavior of the PID curves of MBO can be explained on the basis of the relative values of the tunneling lifetimes from localized tunneling recombination model, and the thermal lifetimes obtained from the delocalized recombination OTOR model. The tunneling lifetimes of 0.38 s and 6.4 s are very low compared with thermal lifetime of 62 s of the first component. In fact thermal lifetimes of the order of 6.4 s exist only for temperatures greater than the peak maximum temperature T_{max}, which for MBO is around 200 °C (473 K). However, this argument has to be verified.

The previous argument can be easily verified by a simple simulation taking into account that from a theoretical point of view, there is an infinite number of (E,s) pairs corresponding to the T_{max}

of 200 °C. A simulation was carried out which searched for (E,s) pairs which would yield a glow peak maximum T_{max} at 200± 2 °C, with the heating rate of 2 °C/s used in the present work. The search was performed in the intervals E[0.8–1.8] eV and s[10^8 – 10^{18}]s^{-1}. The simulation was run for kinetics order $b = 1.05$ and $b = 2$, resulting in 48 (E,s) pairs for each value of b. The values of τ_{max} for $b = 2$ were 10.6 s for the lowest possible (E,s) pair (0.9 eV – 1.1 10^9 s^{-1}), and 5.7 s for the highest possible (E,s) pair (1.75 eV – 8.9 10^{17} s^{-1}). The corresponding values for $b = 1.05$ were by about 10% lower.

Therefore, the thermal lifetimes at the decay temperatures used in the present work (see Fig. 1), are by one and two orders of magnitude greater than the tunneling lifetime of 0.38 s and 6.4 s obtained in this work.

During thermal excitation at a stable temperature the electrons can be either excited to a higher energy level without escaping from the trap, or can escape from the trap into the conduction band, and subsequently they recombine in a luminescence center. When the trap to luminescence center distance is large, only a delocalized transition is observed. However, when the trap to luminescence center distance is small, then a tunneling recombination from the excited state is possible. According to the results of the present work, the trap to luminescence center distance in MBO favors the tunneling recombination. In fact the delocalized behavior is completely absent for decay temperatures up to 140 °C. Above 150 °C the thermal lifetime remains still higher than the tunneling lifetimes, but it becomes of the order of the tunneling lifetime of the second component. This change causes the experimentally observed weak dependence of the lifetimes on the decay temperature T_{dec}.

The behavior of the dimensionless density parameter ρ', which is very important in the model by Jain et al. (2012), is shown in Fig. 12 for both components (C_1 and C_2). The very low value ρ' obtained for component C_2 is probably due to the poor statistics of this component up to a PID temperature of 130 °C. The horizontal straight line with error bars corresponding to the mean value of C_1 and its standard deviation, i.e. $\rho' = 0.0052 \pm 0.0025$, shows again the range within which this parameter can be considered as constant.

6. Concluding remarks

The conclusions of the present work can be summarized as follows:

- Both the TL glow-curves and the PID curves of LBO data are very well described by either the general order expressions representing delocalized radiation transitions, or by the recently developed equations Eq. (5) based on the Lambert function.
- The value of the activation energy resulting from the PID analysis of LBO data, agrees very well with the values obtained by initial rise and CGCD methods of analysis of TL glow curves.
- Both the TL glow-curves and the PID curves of MBO are poorly described by either the analytical general order expression, or by the expression based on the OTOR solution function.
- Both the TL glow-curves and the PID curves of MBO are very well described by the tunneling expressions representing localized radiative transitions given by Eq. (11) and Eq. (15).
- The values of the activation energy derived from the isothermal analysis of MBO are 10% lower than the values obtained by the initial rise and CGCD methods.

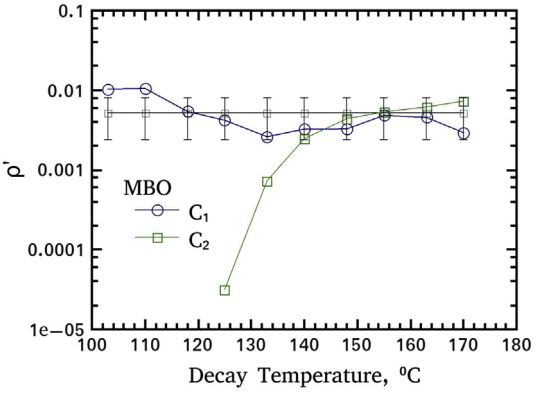

Fig. 12. The values of the parameter ρ' for the two components of the PID curve of MBO. The horizontal straight line with error bars corresponds to the mean value and its standard deviation $\rho' = 0.0052 \pm 0.0025$.

The experimental data for MBO in this paper were analyzed using the model by Jain et al. (2012). However, previous research has shown that band-tail states exist in materials like feldspars and that they play an important role in the production of luminescence signals in these materials. The model by Jain et al. (2012) used in this paper ignores these band-tail states, from which the electrons can recombine with holes via thermal hopping or tunneling (Li and Li (2013); Poolton et al. (2009, 2002a, 2002b)).

It is also noted that in a recent comparative study of several luminescence models for feldspars, Guralnik et al. (2015) discussed three luminescence models for feldspars, and tested these models against isothermal and dose response experimental data. They concluded that all models can provide a reasonable description of the experimental data for their samples.

Based on the different behavior of the isothermal signals of the two dosimeters, it is suggested that isothermal studies of TL at high temperatures can be used to distinguish between materials whose luminescence obey either transitions involving delocalized kinetics, or transitions based on localized recombination processes.

References

Balian, H.G., Eddy, N.W., 1977. Figure Of Merit (FOM): an improved criterion over the normalized chi-square test for assign the goodness-of-fit of gamma ray spectral peaks. Nucl. Instrum. Method 145, 389–395.
Chandra, B., Bhatt, R.C., 1981. Isothermal decay characteristics of $Li_2B_4O_7$:Mn phosphor. Nucl. Instrum. Method B 184, 557–559.
Chen, R., McKeever, S.W.S., 1997. Theory of Thermoluminescence and Related Phenomena. World Scientific.
Corless, R.M., Gonnet, G.H., Hare, D.G.E., Jeffrey, D.J., Knuth, D.E., 1996. On the Lambert W function. Adv. Comput. Math. 5, 329–359.
Doul, B.A., Olivera, D.C., Wang, L.Y., Milliken, E.D., Yukihara, E.G., 2014. Thermoluminescent properties of lithium borate, magnesium borate and calcium sulfate developed for temperature sensing. J. Lumin. 146, 408.
Doull, B.A., Olivera, D.C., Yukihara, E.G., 2013. Effect of annealing and fuel type on the thermoluminescent properties of $Li_2B_4O_7$ synthesized by solution combustion synthesis. Radiat. Meas. 56, 167.
Driscoll, C.M.H., 1981. Sensitivity and fading characteristics of thermoluminescent magnesium borate. Radiat. Prot. Dosim. 1, 135.
Furetta, C., Kitis, G., Wenf, P.S., Chu, T.C., 1999. Thermoluminescence characteristics of *MgB_4O_7:Dy,Na*. Nucl. Instrum. Method Phys. Res. B 420, 441–445.
Furetta, C., Prokic, M., Salamon, R., Kitis, G., 2000. Dosimetric characterization of a new production *MgB_4O_7:Dy,Na*. Appl. Radiat. Isot. 52, 243–250.
Furetta, C., Prokic, M., Salamon, R., Prokic, V., Kitis, G., 2001. Dosimetric characteristics of tissue equivalent thermoluminescent solid TL detectors based on lithium borate. Nucl. Instrum. Method 456, 411–417.
GSL-GNU Scientific Library, 2015. www.gnu.org/software/gsl.
Guralnik, B., Li, B., Jain, M., Chen, R., Paris, R.B., Pagonis, V., Valla, P.G., Herman, F., 2015. Radiation Measurements 81, 224–231. http://dx.doi.org/10.1016/j.radmeas.2015.02.011.
Jain, M., Guralnik, B., Andersen, M.T., 2012. Stimulated luminescence emission from localized recombination in randomly distributed defects. J. Phys. Condens. Matter 24, 385402.
Karali, T., Rowlands, A.P., Prokic, M., Townsend, P.D., Halmagean, E., 2002. Thermoluminescent spectra of rare earth doped MgB_4O_7 dosemeters. Radiat. Prot. Dosim. 100, 191.
Kitis, G., Pagonis, V., 2013. Analytical solutions for stimulated luminescence emission from tunneling recombination in random distribution of defects. J. Lumin.

137, 109–115.
Kitis, G., Pagonis, V., 2014. Properties of thermoluminescence glow curves from tunneling recombinations processes in random distributions of defects. J. Lumin. 153, 118–124.
Kitis, G., Vlachos, N.D., 2012. General semi-analytical expressions for TL, OSL and other luminescence stimulation modes derived from the OTOR model using the Lambert W-function. Radiat. Meas. 48, 47–54.
Kitis, G., Bousbouras, P., Antypas, C., Charalambous, S., 1991. Anomalous fading in apatite. Nucl. Tracks Radiat. Meas. 18, 161–166.
Kitis, G., Gomez Ros, J.M., Tuyn, J.W.N., 1998. Thermoluminescence glow–curve deconvolution function for first, second and general order kinetics. J. Phys. D Appl. Phys. 31, 2636–2641.
Kitis, G., Furetta, C., Prokic, M., Prokic, V., 2000. Kinetic parameters of some tissue equivalent thermoluminescence materials. J. Phys. D Appl.Phys 33, 1252–1262.
Kitis, G., Chen, R., Pagonis, V., Carinou, E., Kamenopoulou, V., 2006. Thermoluminescence under an exponential heating function: I. Theory. J. Phys. D. Appl. Phys. 39, 1500–1507.
Kutomi, Y., Takeuchi, N., 1986. Thermoluminescence in lithium tetraborate doped with activators. J. Mater. Sci. Lett. 5, 51–53.
Kutomi, Y., Takeuchi, M., 1996. The effect of pre-irradiation annealing on TL and PTTL glow curves of pure $Li_2B_4O_7$ single crystals. Radiat. Prot. Dosim. 65, 333–337.
Li, B., Li, S.-H., 2013. The effect of band-tail states on the thermal stability of the infrared stimulated luminescence from K-feldspar. J. Lumin 136, 5.
Lochab, S.P., Pandey, A., Sahare, P.D., Chauhan, R.S., Salah, N., Ranjan, R., 2007. Nanocrystalline MgB4O7:Dy for high dose measurement of gamma radiation. Phys. Status Solidi A 204, 2416.
Martini, M., Meinardi, F., Kovacs, L., Polgar, K., 1996. Spectrally resolved thermoluminescence of Li2B4O7:Cu single crystals. Radiat. Prot. Dosim. 65, 343–346.
May, C.E., Partridge, J.A., 1964. Thermoluminescence kinetics of Alpha-irradiated alkali halides. J. Chem. Phys. 40, 1401–1409.
McKeever, S.W.S., Moscovitch, M., Townsend, P.D., 1995. Thermoluminescence Dosimetry Materials: Properties and Uses. Nuclear Technology Publishing, Ashford.
MINUIT, a Physics Analysis Tool for Function Minimization. Released in ROOT, 2015.
Pagonis, V., Morthekai, P., Kitis, G., 2014. Kinetic analysis of thermoluminescence glow curves in feldspar: evidence of a continuous distribution of energies. Geochronometria 41 (2), 168–177.
Park, K.S., Ahn, J.K., Kim, D.J., Kim, H.K., Hwang, Y.H., Kim, D.S., Park, M.H., Park, Y., Yoon, J.J., Leem, Y.J., 2003. Growth and properties of $Li_2B_4O_7$ single crystals doped with Cu, Mn and Mg. J. Cryst. Growth 249, 483–486.
Poolton, N.R.J., Wallinga, J., Murray, A.S., Bulur, E., Bøtter-Jensen, L., 2002a. Electrons in feldspar I: on the wavefunction of electrons trapped at simple lattice defects. Phys. Chem. Miner. 29, 210.
Poolton, N.R.J., Ozanyan, K.B., Wallinga, J., Murray, A.S., Bøtter-Jensen, L., 2002b. Electrons in feldspar II: a consideration of the influence of conduction band-tail states on luminescence processes. Phys. Chem. Miner. 29, 217.
Poolton, N.R.J., Kars, R.H., Wallinga, J., Bos, A.J.J., 2009. Direct evidence for the participation of band-tails and excited-state tunneling in the luminescence of irradiated feldspars. J. Phys. Condens. Matter 21 art.no. 485505.
Price, J.L., Guardala, N.A., Riel, G.K., Mathur, V.K., 1998. Neutron response of a laser-heated thermoluminescence dosimetry system. Radiat. Meas. 29, 379.
Prokic, M., 1980. Development of highly sensitive $CaSO_4$:Dy/Tm and MgB_4O_7:Dy,Tm sintered thermoluminescent dosimeters. Nucl. Instrum. Methods 175, 83.
Prokic, M., 2001a. Lithium borate solid TL detectors. Radiat. Meas. 33, 393–396.
Prokic, M., 2001b. Dosimetric characteristics of $Li_2B_4O_7$:Cu, Ag, P solid TL detectors. Radiat. Prot. Dosim. 100, 265–268.
Prokic, M., 2007. Individual monitoring based on magnesium borate. Radiat. Prot. Dosim. 125, 247.
Prokic, M., Bøtter-Jensen, L., 1993. Comparison of main thermoluminescent properties of some TL dosemeters. Radiat. Prot. Dosim. 47, 195.
Prokic, M., 1993. MgB_4O_7:Mn as a new TL dosemeter. Radiat. Prot. Dosim. 47, 191.
ROOT, A Data Analysis Framework, 2015. https://root.cern.ch.
Sadek, A.M., Eissa, H.M., Basha, A.M., Carinou, E., Askounis, P., Kitis, G., 2015. The deconvolution of thermoluminescence glow curves using general expressions derived from one trap-one recombination (OTOR) level model. Appl. Radiat. Isot. 95, 214–221.
Sfampa, I.K., Polymeris, G.S., Tsirliganis, N.C., Pagonis, V., Kitis, G., 2014. Prompt isothermal decay of thermoluminescence in an apatite exhibiting strong anomalous fading. Nucl. Instrum. Method Phys. Res. B 320, 57–63.
Sfampa, I.K., Polymeris, G.S., Pagonis, V., Theodosoglou, E., Tsirliganis, N.C., Kitis, G., 2015. Correlations of basic TL,OSL and IRSL properties of ten K-feldspqr samples of various origin. Nucl. Instrum. Method Phys. Res. B 359, 89–98.
Takenaga, M., Yamamota, O., Yamashita, T., 1980. Preparation and characteristics of Li2B4O7:Cu phosphor. Nucl. Instrum. Method 175, 77–78.
Tiwari, B., Rawat, N.S., Desai, D.G., Singh, S.G., Tyagi, M., Ratna, P., Gadkari, S.C., Kulkarni, M.S., 2010. Thermoluminescence studies on Cu-doped $Li_2B_4O_7$ single crystals. J. Lumin. 130, 2076–2083.
Visocekas, R., Ceva, T., Marti, C., Lafaucheux, F., Roberts, M.C., 1976. Tunneling radiative recombination in labradorite: its association with anomalous fading in thermoluminescence. Phys. Status Sol.(a) 35, 315–327.
Wall, B.F., Driscoll, C.M.H., Stong, J.C., Fisher, E.S., 1982. The suitability of different preparations of thermoluminescent lithium borate for medical dosimetry. Phys. Med. Biol. 27, 1023–1034.
Wintle, A.G., 1977. Detailed study of minerals exhibiting anomalous fading. J. Lumin. 15, 385–393.
Yukihara, E.G., Milliken, E.D., Doull, B.A., 2014a. Thermally stimulated and recombination processes in MgB4O7 investigated by systematic lanthanide doping. J. Lumin. 154, 251.
Yukihara, E.G., Colleman, A.C., Doull, B., 2014b. Passive temperature sensing using thermoluminescence: laboratory tests using $Li_2B_4O_7$:Cu,Ag, MgB_4O_7:Dy,Li and $CaSO_4$:Ce,Tb. J. Lumin. 146, 515.